FULL PAPER

Dalton
www.rsc.org/dalton

One- and two-dimensional coordination assemblies of a novel redox-active bipyridinium dimer ligand with magnetic oxalate complexes †

Yan-Qiong Sun, Jie Zhang * and Guo-Yu Yang
State Key Laboratory of Structural Chemistry, Fujian Institute of Research on the Structure of Matter, Chinese Academy of Sciences, Fuzhou, Fujian 350002, China.
E-mail: zhangjie@ms.fjirsm.ac.cn

Received 19th May 2003, Accepted 24th July 2003
First published as an Advance Article on the web 11th August 2003

The synthesis of a novel redox-active bipyridinium dimer ligand, 1,4-bis(4′-pyridyl-1′-pyridinio)phthalazine (**Bpyph**) dichloride and its magnetic coordination assemblies [(**Bpyph**)$Cu^{II}Fe^{II}(C_2O_4)_3$]·6.5H_2O (**1**) and [(**Bpyph**)$Co^{II}_2(C_2O_4)_3$]·5.5H_2O (**2**) are described. X-Ray single-crystal diffraction studies confirm that compound **1** is built from $[CuFe(C_2O_4)_3]^{2-}$ units bridged sequentially by **Bpyph** cations to form polymeric chains with Δ and Λ enantiomers in $[Fe(C_2O_4)_3]^{4-}$. Compound **2** consists of honeycomb layers of the cobalt oxalate complex $[Co_2(C_2O_4)_3]^{2-}$ interleaved by **Bpyph** cations. The magnetic susceptibility data show antiferromagnetic interaction in both compounds with Weiss constants −2.38 K for **1** and −38 K for **2**.

Introduction

An important goal in coordination chemistry is the rational design of functional molecular materials that exhibit potential applications such as redox-activity, electro-chromic displays, prototypical electron-transfer, ferromagnetic and non-linear optical (NLO) properties. Because the coexistence of two functions in the same crystal lattice might result in new physical phenomena and novel applications, a promising strategy in the field of molecular materials is to create "bi-functional" hybrid organic/inorganic compounds by self-assembly techniques.[1] In the construction of multifunctional materials, oxalate-bridged polynuclear complexes play a key role due to the remarkable ability of the oxalate ligand to transmit electronic effects between magnetic centers[2,3] and the wide variety of topologies for the coordination geometries of the oxalate anion with different metal ions.[4,5] There have been some examples which show that π-conjugated donor molecules such as tetrathiafulvalene (TTF),[6,7] redox-active decamethylmetallocenium,[8] as well as NLO cations[9] assembled with oxalate-bridged anions, exhibit the coexistence of magnetism and conductivity/non-linear optical properties. But few reports are found of assemblies of viologen derivatives with oxalate anionic complexes. In view of the versatility of viologen derivatives in redox mediators, display materials, electrical and ionic conductors and spin-tunable magnetic materials,[10–12] it is expected that a combination of viologen acceptor and oxalate-bridged anionic donor could create new hybrid molecular materials with interesting properties and is useful for exploring important structure–property relationships. Along this line, we have designed and synthesized a novel redox-active phthalazylene-conjugated pyridinium dimer (Scheme 1), 1,4-bis(4′-pyridyl-1′-pyridinio)-phthalazine (**Bpyph**) dichloride as a derivative of the viologen ligand. A one-dimensional coordination polymer, [(**Bpyph**)-$Cu^{II}Fe^{II}(C_2O_4)_3$]·6.5H_2O (**1**) and a two-dimensional polymer complex [(**Bpyph**)$Co^{II}_2(C_2O_4)_3$]·5.5H_2O (**2**) were first obtained by assembling **Bpyph**Cl_2 with oxalate complexes. This paper described the syntheses and characterization of these two magnetic complexes.

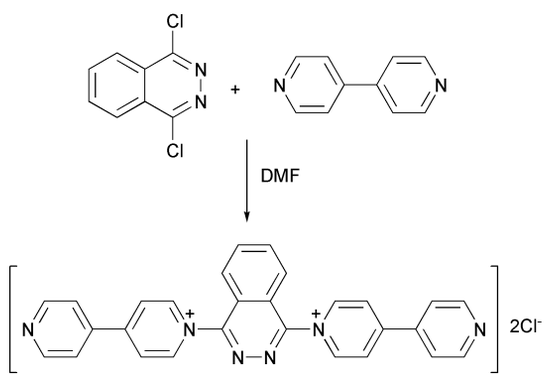

Scheme 1

Experimental

Preparation of the ligand

BpyphCl_2. Phthalaz-1,4-dione and 1,4-dichlorophthalazine were prepared according to the literature methods.[13,14] A mixture of 4,4′-bipyridine (3.85 g, 25 mmol) and 1,4-dichlorophthalazine (1 g, 5 mmol) was dissolved in 8 ml DMF. After stirring at 120 °C under nitrogen for 8 h, the solution was concentrated to a small volume under reduced pressure. Then an excess amount of hot benzene was added, the precipitate was collected by filtration, washed with hot benzene and dried under vacuum to afford a pale green powder (2.48 g, 96.5%). IR (KBr, cm^{-1}): 3382(s), 3107(w), 3031(w), 1633(vs), 1592(m), 1536(m), 1453(m), 1407(s), 1360(vs), 1291(m), 1214(m), 996(w), 870(vs), 669(w), 614(w), 538(w), 486(w); ^1H NMR ($CDCl_3$, ppm): δ 8.19 (4H, d); 8.29 (2H, q); 8.51 (2H, t); 8.93 (8H, d); 9.70 (4H, d).

Preparation of the complexes

[(Bpyph)$Cu^{II}Fe^{II}(C_2O_4)_3$]·6.5H_2O (1). A mixture of **Bpyph**Cl_2 (102.2 mg, 0.2 mmol) and $CuCl_2$ (34 mg, 0.2 mmol) was dissolved in water and then filtered. The resulting filtrate was layered with a H_2O/DMSO (5 : 1,v/v) solution (20 ml) of $(NH_4)_3$-$Fe(C_2O_4)_3$ (85.6 mg, 0.2 mmol) in a 1 : 1 ratio in a straight glass tube. Red-brown needle crystals were obtained by slow interface diffusion after a few days in 45% yield. Found: C, 42.87; H, 2.63; N, 8.61%. $C_{34}H_{33}CuFeN_6O_{18.5}$ requires C, 43.39; H, 3.53; N, 8.93%. IR (KBr, cm^{-1}): 3423(w), 3109(w), 3039(w),

† Electronic supplementary information (ESI) available: IR and ^1H NMR spectra for **Bpyph**Cl_2; IR and ESR spectra for **1**; IR spectrum for **2**; differing chirality of $[Fe(ox)_3]^{4-}$ in **1**; different chiral subunits of **2**; TGA for **1** and **2**; selected bond lengths and angles for **1** and **2**; O ··· O distances in **1** and **2**. See http://www.rsc.org/suppdata/dt/b3/b305560d/

DOI: 10.1039/b305560d

Table 1 Crystallographic data for complexes **1** and **2**

	1	**2**
Empirical formula	$C_{34}H_{33}CuFeN_6O_{18.5}$	$C_{34}H_{31}Co_2N_6O_{17.5}$
Formula weight	941.05	921.51
Crystal system	Monoclinic	Monoclinic
Space group	$P2_1/n$	$P2_1/n$
T/K	293	293
a/Å	12.0458(5)	9.1401(7)
b/Å	15.2355(4)	16.9414(13)
c/Å	21.0978(9)	24.0854(19)
β/°	95.409(2)	90.974(2)
V/Å^3	3854.7(3)	3729.0(5)
Z	4	4
D_c/g cm^{-3}	1.622	1.641
μ/cm^{-1}	10.17	9.78
F(000)	1928	1884
Measured reflections	11967	11625
Independent reflections	6423 [R(int) = 0.0805]	6163 [R(int) = 0.0585]
Goodness-of-fit on F^2	1.005	1.158
R_1 [$I>2\sigma(I)$]	0.0758	0.0855
wR_2 [$I>2\sigma(I)$]	0.1576	0.1438

1716(s), 1682(vs), 1642(s), 1389(s), 1372(s), 1361(s), 1215(w), 1180(w), 888(m), 821(m), 803(m), 720(w), 694(w), 532(m), 500(m).

[(Bpyph)$Co^{II}_2(C_2O_4)_3$]·5.5H_2O (2). The filtrate of an aqueous solution (20 ml) of **Bpyph**Cl_2 (102.2 mg, 0.2 mmol) and $K_2C_2O_4$(110.5 mg, 0.6 mmol) was layered with a H_2O/DMSO (5 : 1,v/v) solution (20 ml) of $CoCl_2$ (48 mg, 0.4 mmol) in a 1 : 1 ratio in a straight glass tube. Red single crystals were obtained by slow diffusion after a few days in a yield of 41%. Found: C, 43.92; H, 3.47; N, 8.74%. $C_{34}H_{31}Co_2N_6O_{17.5}$ requires C, 44.31; H, 3.39; N, 9.12%. IR (KBr, cm^{-1}): 3426(w), 3120(w), 3062(w), 1636(s), 1601(vs), 1458(m), 1406(m), 1357(s), 1310(m), 1216(w), 1183(w), 822(m), 805(s), 772(w), 674(m), 480(m), 528(m).

Crystallography

The intensity data were collected on a Smart CCD diffractometer with graphite-monochromated Mo-Kα (λ = 0.71073 Å) radiation at room temperature. All absorption corrections were performed using the SADABS program.[15] The structure solution and refinement were carried out using the SHELX suite of programs.[16,17] All non-hydrogen atoms were refined anisotropically except for the oxygen atoms of the free water molecules. All hydrogen atoms were generated geometrically (C–H 0.96 Å) with the exception of the hydrogen atoms of the free water molecules. Experimental X-ray data for complexes **1** and **2** are listed in Table 1. Selected bond lengths and angles are given as ESI.†

CCDC reference numbers 210901 and 210902.

See http://www.rsc.org/suppdata/dt/b3/b305560d/ for crystallographic data in CIF or other electronic format.

Physical measurements

The elemental analyses were determined on a Vario EL *III* CHNOS elemental analyzer. Thermogravimetric data were collected on a Mettler Toledo TGA/SDTA 851^e analyzer in flowing nitrogen at a heating rate of 5 °C min^{-1}. IR spectra were recorded on a Bomem BM102 FT-IR spectrometer with KBr pellets. ESR spectroscopy was performed at X-band frequency with a Bruker ER-420 spectrometer. Variable-temperature magnetic susceptibilities were measured from 300 to 5 K at a 1.0 T external field using a Quantum Design MPMS-7 magnetometer, the susceptibility of the sample holder and the diamagnetic contribution (502 × 10^{-6} cm^3 mol^{-1}) was subtracted from the raw data for the two complexes.

Results and discussion

Crystal structures

[(Bpyph)$Cu^{II}Fe^{II}(C_2O_4)_3$]·6.5H_2O (1). The crystal structure of complex **1** consists of one-dimensional chains in which $[CuFe(C_2O_4)_3]^{2-}$ units are bridged sequentially by asymmetric **Bpyph** cations (Fig. 1). One copper centre and one iron centre are crystallographically distinguishable. The iron centre exhibits a +2 oxidation state in the complex attributed to a reductive reaction during molecular assembly, which is similar to the case of $[Fe^{II}_3(C_2O_4)_3(4,4'\text{-bpy})_4]$[18] and can be proved by a characteristic ESR signal at g = 2.13, typical for a Cu^{II} site, without providing information on the Fe^{III} species.[19] The Cu atom lying in a general position, is coordinated by two nitrogen atoms from two **Bpyph** ligands and two oxygen atoms from the same oxalate anion in a distorted tetrahedral geometry. The O–Cu–O(N) bond angles range from 69.4(2) to 100.6(2)°. The Cu1–O1, Cu1–O2, Cu1–N1A and Cu1–N2 bond length are 2.432(6), 2.424(6),1.927(5) and 1.938(6) Å. **Bpyph**$^{2+}$ is almost linear and acts as a bidentate ligand to link the two copper centres *via* two terminal nitrogen atoms with a N1A–Cu1–N2 bond angle of 163.3(3)°. There is a unique bridging oxalate ligand chelating the copper and iron centres *via* its oxygen atoms. The FeO_6 chromophore in a general position must be described as a slightly distorted octahedron with Fe–O bond distances ranging from 1.972(6) to 2.027(5) Å, and O–Fe–O bond angles between 80.2(2) and 98.6(2)°. Six oxygen atoms come from three crystallographically independent oxalato ligands among which there are two terminal bidentate ones and one bis-bidentate one. $[Fe(C_2O_4)_3]^{4-}$ fragments are attached to the 1-D chain by the bridging oxalate ligands as branches on the same side of the chain in Δ or Λ enantiomeric forms. In the packing diagram (Fig. 2), chain 1 and chain 2 in a sequence of four chains are related by a *n* glide plane perpendicular to the *b*/2 axis. Chain 3 is related to chain 1 by a two-fold screw axis parallel to the *b* axis while chain 4 is symmetry related to chain 1 by inversion.

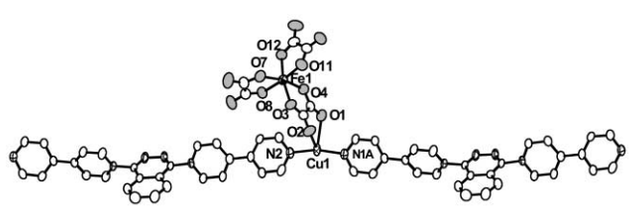

Fig. 1 ORTEP[26] drawing (50% probability level) with the atom-numbering scheme for complex **1**, [(**Bpyph**)$CuFe(C_2O_4)_3$]·6.5H_2O. The H atoms are omitted for clarity.

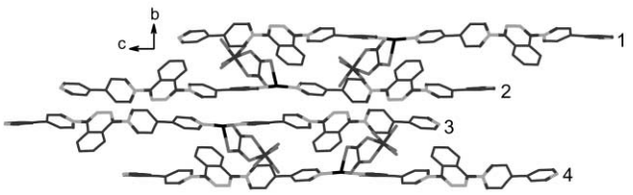

Fig. 2 The packing structure for complex **1** [(**Bpyph**)CuFe(C_2O_4)$_3$]·6.5H_2O along the *a*-axis. The H atoms and crystalline water molecules are omitted for clarity.

The two pyridyl rings in the two 4,4′-bipyridine groups of **Bpyph**$^{2+}$ are non-planar (the dihedral angles are 25.8(2) and 33.5(4)°). The phthalazine ring is closely perpendicular to the two neighbouring pyridyl rings with dihedral angles of 72.8(2) and 77.5(2)°. Adjacent layers stack over one another in a staggered fashion, and are held together by hydrogen bonds between the water molecules and oxalate ligands (O ··· O distances: 2.507(27)–3.019(13) Å), thus yielding a 3-D extended network while the distance between two adjacent layers is 3.81 Å.

[(Bpyph)Co$^{II}_2$(C_2O_4)$_3$]·5.5H_2O (2). The crystal structure of **2** consists of a homometallic, anionic two-dimensional network with stoichiometry [$Co_2(C_2O_4)_3]^{2-}$, which is interleaved by organic layers of **Bpyph**$^{2+}$ cations. A perspective view of the asymmetric unit of **2** containing two Co^{II}, three oxalate ligands and one **Bpyph**$^{2+}$ cation is shown in Fig. 3. The Co^{II} ions are octahedrally surrounded by three bis(chelating) oxalate ligands. The Co–O bond lengths ranging from 2.110(6) to 2.146(5) Å are slightly longer than the values in the tris-oxalate Co^{II} anionic 3-D network (average value 2.076 Å),[20] but are within the range of Co–O bond lengths observed in [Co^{II}_2(HPO_4)-(C_2O_4)]$^-$ anions (from 2.070 to 2.212 Å).[21] The two crystallographically independent Co1 and Co2 alternately are connected through ambient oxalate ligands to form honeycomb homometallic layers in the *ab* plane (Fig. 4a). Each anion layer contains Co1 and Co2 tris(oxalate) sites of opposite configuration (Δ and Λ) arranged in alternating rows with a . . . ΔΛ–ΛΔ–ΔΛ–ΛΔ . . . pattern (where – represents segregation between layers). This alternating construction of different chiral subunits is similar to that observed in the 2-D honeycomb bimetallic layer structure of formula X[$M^{II}M^{III}$(C_2O_4)$_3$] (X = cation).[22]

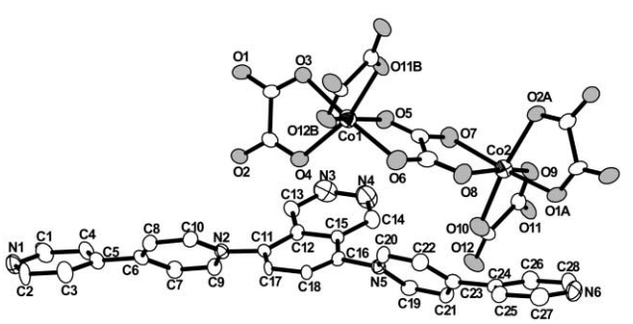

Fig. 3 ORTEP drawing (50% probability level) with the atom-numbering scheme for complex **2**, [(**Bpyph**)$Co_2(C_2O_4)_3$]·5.5H_2O. The H atoms are omitted for clarity.

The interleaving organic layers are constructed from one crystallographically independent **Bpyph**$^{2+}$ cation located in a general position. The **Bpyph**$^{2+}$ cation is non-planar, the angles between the adjacent pyridyl rings being 38.0(3) and 38.9(3)°, at the same time the mean plane of the phthalazine ring is also twisted out of the plane of the adjacent pyridyl ring by 50.7(2) and 59.4(3)°. In every organic layer, all of the cations are related by inversion centres or translations, the pyridazyl group of each **Bpyph**$^{2+}$ points to the anionic layers while fitting into the centre of a vacancy, and retaining a long molecular chain parallel to the honeycomb layer (Fig. 4b). Since there is no H-bonding between the anions and cations, the "docking" of the pyridazyl groups into the cavities between the anions is a crucial consideration in templating the present packing arrangement and stabilizing the lattice. Further H-bonding between the free water molecules and the O atoms of [$Co_2(ox)_3]^{2-}$ or N atoms of **Bpyph**$^{2+}$ link the anionic layers into a 3-D network.

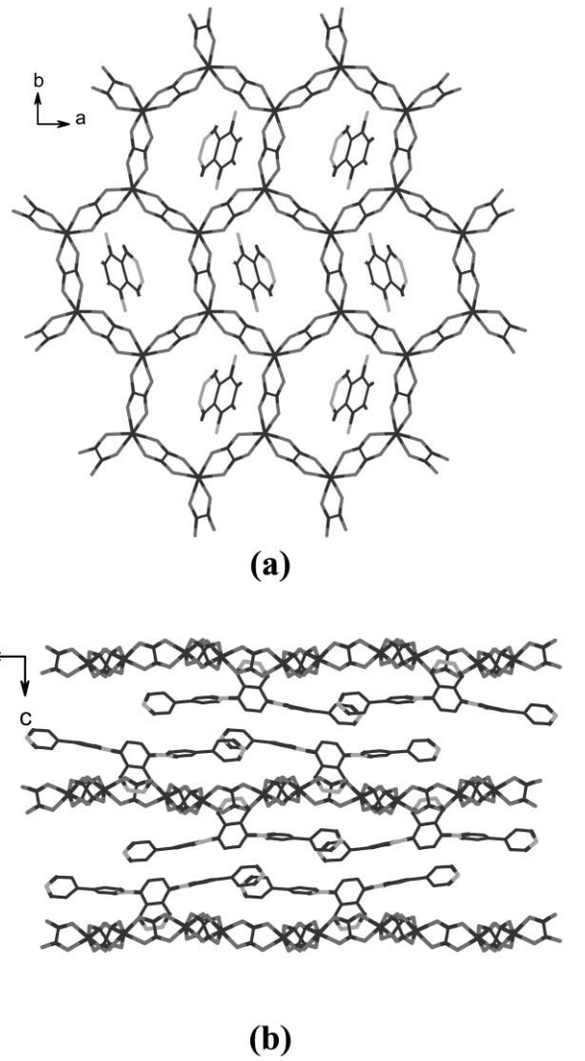

Fig. 4 (a) View of the structure in the *ab* plane showing the honeycomb magnetic layers. (b) Representation of the hybrid structure along the *c*-axis, showing the alternating organic/inorganic layers of complex **2**, [(**Bpyph**)$Co_2(C_2O_4)_3$]·5.5H_2O. The H atoms and crystalline water molecules are omitted for clarity.

Thermal properties

The thermal stability of complexes **1** and **2** was determined by thermogravimetric analysis (TGA). For **1**, the first weight loss of 13.27% from 30 to 135 °C corresponds to the loss of free water molecules (calc.12.44%). The second weight loss of 55.62% is observed from 135 to 464 °C, which is attributed to the removal of one **Bpyph**$^{2+}$ cation and one oxalate anion per formula unit (calc. 56.11%). After 464 °C, the residual oxalate of complex **1** starts to decompose and converts to oxide above 800 °C. For **2**, the initial weight loss of 11.56% from 30 to 163 °C is close to the release of free water molecules (calc. 10.75%). After 163 °C, complex **2** begins to decompose. Between 163 and 578 °C, the second weight loss of 64.57% corresponds to the removal of the **Bpyph**$^{2+}$ cation and one oxalate anion and the decomposition of one oxalate per formula unit (calc. 65.11%). After 578 °C, the residual oxalate of complex **2** decomposes completely and converts to oxide above 800 °C.

Magnetic properties

The thermal variation of the magnetic susceptibility in the form of a reciprocal molar susceptibility ($1/\chi_M$) and $\chi_M T$ *versus* temperature (T) for complex **1**, is shown in Fig. 5. The plot of $\chi_M T$ *vs.* T shows a continuous decrease on cooling from room temperature, but shows a small increase at about 9 K, followed by a sharp decrease at lower temperatures. At 300 K the effective magnetic moment (μ_{eff}) per formula, determined from the equation $\mu_{eff} = 2.828(\chi_M T)^{1/2}$, is 6.09 μ_B which is higher than the sum of the expected contributions (5.19 μ_B) for two isolated Cu^{II} (S = 1/2) and high-spin Fe^{II} (S = 2) centers, indicating an important orbital contribution is involved. The Cu^{II} center in compound **1** can contribute 1.84 μ_B (calculated from g = 2.13 by ESR measurement) to the total observed magnetic moment of 6.09 μ_B, so a magnetic moment of 5.80 μ_B is expected for the S = 2 iron with an appreciable orbital contribution, which is close to the effective magnetic moment of 5.68 μ_B for $[Fe^{II}_3(C_2O_4)_3(4,4'\text{-bpy})_4]$.[18] Above 40 K the variation of $1/\chi_M$ is well described by the Curie–Weiss law $1/\chi_M = (T - \theta)/C$ to give a negative Weiss constant (θ = −2.38 K), indicating a weak antiferromagnetic interaction between the paramagnetic centers.

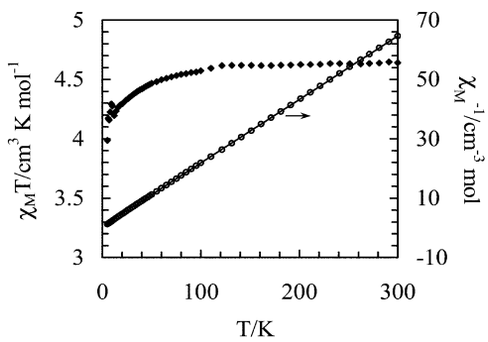

Fig. 5 The temperature dependences of reciprocal magnetic susceptibility χ_M^{-1} (○) and the product $\chi_M T$ (◆) for complex **1**, [(**Bpyph**)$CuFe(C_2O_4)_3$]·$6.5H_2O$.

The magnetic susceptibility data for complex **2** are plotted in Fig. 6 as both χ_M and $\chi_M T$ *vs.* T**.** The effective magnetic moment per cobalt (5.51 μ_B) at room temperature is obviously greater than the spin-only value of 3.87 μ_B for the high spin Co^{II} center (S = 3/2). This higher value is close to those reported for oxalate-bridged cobalt(II) complexes (μ_{eff} ranges from 5.02 to 5.45 μ_B) and can be attributed to the orbital contribution of the Co^{II} center.[18,23] Upon cooling, χ_M increases to a maximum around 10 K, suggesting the presence of antiferromagnetic coupling in the anionic 2-D coordination polymer. This dominant antiferromagnetic character is confirmed by a negative Weiss constant (−38 K) obtained from fitting the data in the temperature range 30–300 K using the Curie–Weiss equation.

The chain structures of compound **1** contain metal(II) oxalate dimers linked by **Bpyph** molecules. There are two possible

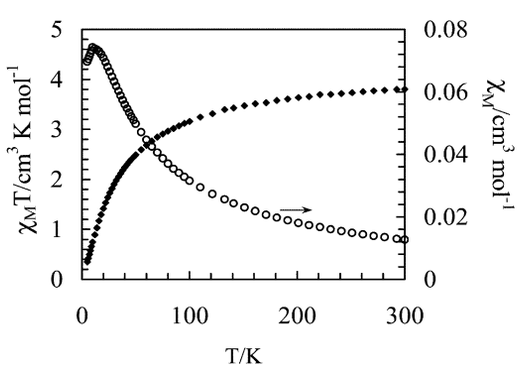

Fig. 6 The temperature dependences of magnetic susceptibility χ_M (○) and the product $\chi_M T$ (◆) for complex **2**, [(**Bpyph**)$Co_2(C_2O_4)_3$]·$5.5H_2O$.

pathways in mediating the magnetic coupling between the paramagnetic metal centers: one is through a **Bpyph** coupler and the other is through the oxalate bridge. Since the Cu ··· Cu distances between the **Bpyph** bridges over the 1-D chain is *ca.* 23.28 Å, the magnetic interaction through the first pathway is expected to be very weak, and this interaction could be further reduced due to the twist of the two pyridine rings of the **Bpyph** molecule. It is well known that an efficient magnetic exchange can be transported through the oxalate bridge,[2,3] therefore, the observed antiferromagnetic interaction could be mainly attributed to the exchange coupling between the Cu^{II} and Fe^{II} ions through the oxalate bridge. The susceptibility data were therefore analyzed using an expression[24] for an S = 1/2, S = 2 binuclear spin system based on the Heisenberg Hamiltonian $H = -2JS_a \times S_b$. However, the observed and calculated values do not fit satisfactorily, especially at low temperatures (<30 K). The inclusion of an intrachain exchange based on the molecular field approximation does not improve the theoretical fitting obviously. The Fe^{II} ions have complex electronic ground states, they generally show a large zero-field splitting as well as single-ion anisotropy due to spin–orbit coupling,[25] which results in the magnetic data being difficult to reproduce using an isotropic Heisenberg spin-exchange operator even if axial zero-field splitting is considered.

The magnetic properties of compound **2** completely originate from the strong Co–Co exchange interaction through the extended oxalate bridge. To the best of our knowledge, this is the first example of a homometallic oxalate bridge honeycomb layer constructed of Co^{II} ions. Different from most two-dimensional bimetallic oxalate-bridge network showing ferromagnetic or ferrimagnetic interactions, compound **2** exhibits an obvious antiferromagnetic coupling due to an efficient exchange interaction occurring between two magnetic orbitals of the same symmetry.

Conclusions

This paper reports two novel coordination polymers [(**Bpyph**)-$Cu^{II}Fe^{II}(C_2O_4)_3$]·$6.5H_2O$ (**1**) and [(**Bpyph**)$Co^{II}_2(C_2O_4)_3$]·$5.5H_2O$ (**2**), obtained by assembling redox-active **Bpyph**Cl_2 ligands with oxalate complexes. The various assembly modes of **Bpyph** with magnetic anionic donors provide a great potential in constructing multifunctional organic/inorganic hybrid materials and establishing important structure–property relationships. More physical properties and further assemblies of the **Bpyph** ligand with other anionic donors are in progress.

Acknowledgements

The authors acknowledge the financial support of the Natural Science Foundation of China (No.20201010), the Natural Science Foundation of Fujian Province of China (No. E0220003/2001J022), the Ministry of Education, and the Ministry of Personnel of China.

Notes and references

1 F. Palacio and J. S. Miller, *Nature (London)*, 2000, **408**, 421; J. M. Lehn, *Supramolecular Chemistry: Concepts and Perspectives*, VCH, Veinheim, 1995; M. D. Ward, *Chem. Soc. Rev.*, 1995, **24**, 121.

2 G. Ballester, E. Coronado, C. Giménez-Saiz and F. Romero, *Angew. Chem., Int. Ed.*, 2001, **40**, 792; I. Castro, L. Calatayud, J. Sletten, F. Lloret and M. Julve, *J. Chem. Soc., Dalton Trans.*, 1997, 811.

3 A. Gleizes, M. Julve, M. Verdaguer, J. A. Real, J. Faus and X. Solans, *J. Chem. Soc., Dalton Trans.*, 1992, 3209; M. Julve, J. Faus, M. Verdaguer and A. Gleizes, *J. Am. Chem. Soc.*, 1984, **106**, 8308; O. Khan, *Angew. Chem., Int. Ed. Engl.*, 1985, **24**, 834.

4 S. Rashid, S. S. Turner, D. Le Pevelen, P. Day, M. E. Light, M. B. Hursthouse, S. Firth and R. J. H. Clark, *Inorg. Chem.*, 2001, **40**, 5304; P. Farrell, T. W. Hambley and P. A. Lay, *Inorg. Chem.*, 1995, **34**, 757; S. G. Carling, C. Mathoniere, P. Day, K. M. A. Malik,

S. J. Coles and M. B. Hursthouse, *J. Chem. Soc., Dalton. Trans.*, 1996, 1839; R. Pellaux, H. W. Schmalle, R. Huber, P. Fischer, T. Hauss, B. Ouladdiaf and S. Decurtins, *Inorg. Chem.*, 1997, **36**, 2301.
5 S. Decurtins, H. W. Schmalle, P. Schneuwyl, J. Ensling and P. Gütlich, *J. Am. Chem. Soc.*, 1994, **116**, 9521; R. Andrés, M. Gruselle, B. Malézieux, M. Verdaguer and J. Vaissermann, *Inorg. Chem.*, 1999, **38**, 4637.
6 H. Akutsu, A. Akutsu-Sato, S. S. Turner, D. LePevelen, P. Day, V. Laukhin, A. K. Klehe, J. Singleton, D. A. Tocher, M. R. Probert and J. A. K. Howard, *J. Am. Chem. Soc.*, 2002, **124**, 12430; L. Martin, S. S. Turner, P. Day, P. Guionneau, J. A. K. Howard, D. E. Hibbs, M. E. Light, M. B. Hursthouse, M. Uruich and K. Yakushi, *Inorg. Chem.*, 2001, **40**, 1363; M. Kurmoo, A. W. Graham, P. Day, S. J. Coles, M. B. Hursthous, J. L. Caulfield, J. Singleton, F. L. Pratt, W. Hayes, L. Ducasse and P. Guionneau, *J. Am. Chem. Soc.*, 1995, **117**, 12209.
7 E. Coronado, J. R. Galán-Mascarós, C. J. Gómez-García and V. Laukhin, *Nature (London)*, 2000, **408**, 447.
8 M. Clemente-León, E. Coronado, J.-R. Galán-Mascarós and C. J. Gómez-García, *Chem. Commun.*, 1997, 1727; E. Coronado, J.-R. Galán-Mascarós, C.-J. Gómez-García, J. Ensling and P. Gütlich, *Chem. Eur. J.*, 2000, **6**, 552.
9 P. G. Lacroix and I. Malfant, *Chem. Mater.*, 2001, **13**, 441; S. Bernard, P. Yu, T. Coradin, E. Rivière, K. Nakatani and R. Cloément, *Adv. Mater.*, 1997, **9**, 981.
10 W. Ong and A. E. Kaifer, *J. Am. Chem. Soc.*, 2002, **124**, 9358; Z. J. Tang and A. M. Guloy, *J. Am. Chem. Soc.*, 1999, **121**, 452; Z. J. Tang, A. P. Litvinchuk, H.-G. Lee and A. M. Guloy, *Inorg. Chem.*, 1998, **37**, 4752.
11 A. Bose, P. He, C. Liu, B. D. Ellman, R. J. Twieg and S. D. Huang, *J. Am. Chem. Soc.*, 2002, **124**, 4.
12 T. Iyoda, M. M. Matsushita and T. Kawai, *Pure Appl. Chem.*, 1999, **71**, 2079; J. Zhang, M. M. Matsushita, X. X. Kong, J. Abe and T. Iyoda, *J. Am. Chem. Soc.*, 2001, **123**, 12105.
13 H. D. K. Drew and H. H. Hatt, *J. Chem. Soc.*, 1936, 16.
14 A. Hirsch and D. Orphanos, *Can. J. Chem.*, 1965, **43**, 2708.
15 G. M. Sheldrick, SADABS, Program for Empirical Absorption Correction of Area Detector Data, University of Göttingen, Germany, 1996.
16 G. M. Sheldrick, SHELXS 97, Program for Crystal Structure Solution, University of Göttingen, Germany, 1996.
17 G. M. Sheldrick, SHELXL 97, Program for Crystal Structure Refinement, University of Göttingen, Germany, 1996.
18 L. M. Zheng, X. Fang, K. H. Lii, H. H. Song, X. X. Xin, H. K. Fun, K. Chinnakali and I. A. Razak, *J. Chem. Soc., Dalton Trans.*, 1999, 2311.
19 Fe^{III} complexes generally display characteristic ESR signals at $g \approx 4$ or $g \approx 6$ for high-spin systems, or $g \approx 2$ assigned to high or low-spin systems.[19a–d] However, the ESR spectrum of complex **1** in a polycrystalline state only exhibits a broad weak signal centered at $g = 2.13$, there are no other spectral features identifiable with an $S = 5/2$ or 1/2 spin state of Fe^{III}. Thus $g = 2.13$ is in good agreement with the presence of a Cu^{II} cation,[19e] and the absence of ESR signals for Fe^{III} species suggests a reduction of Fe^{III} to Fe^{II} which is generally expected to be ESR-silent owing to the relatively large zero-field splitting usually found for high-spin iron^{II}.[19f] An appreciable loss of ESR intensity and relaxation broadening further indicate a dipolar interaction associated with a high-spin Fe^{II} center, which is quite similer to the case of the Cu^{II}–Fe^{II} system.[19f,g] Combined with the structural analysis and the measurement of magnetic susceptibility, it is reasonable to draw a conclusion that the oxidation state of the iron in complex **1** is +2 though the starting material is a Fe^{III} compound. Refer to: (*a*) D. Collison and A. K. Powell, *Inorg. Chem.*, 1990, **29**, 4735; (*b*) J. P. Costes, F. Dahan and J. P. Laurent, *Inorg. Chem.*, 1990, **29**, 2448; (*c*) B. Bazán, J. L. Mesa, J. L. Pizarro, L. Lezama, M. I. Arriortua and T. Rojo, *Inorg. Chem.*, 2000, **39**, 6056; (*d*) S. E. Dessens, C. L. Merrill, R. J. Saxton, R. L. Ilaria, Jr., J. W. Lindsey and L. J. Wilson, *J. Am. Chem. Soc.*, 1982, **104**, 4357; (*e*) N. Singh, S. Gupta and R. K. Sinha, *Inorg. Chem. Commum.*, 2003, **6**, 416; (*f*) R. H. Petty, B. R. Welch, L. J. Wilson, L. A. Bottomley and K. M. Kadish, *J. Am. Chem. Soc.*, 1980, **102**, 611; (*g*) G. A. Brewer and E. Sinn, *Inorg. Chem.*, 1987, **26**, 1529.
20 M. Hernandez-Molina, F. Lloret, C. Ruiz-Perez and M. Julve, *Inorg. Chem.*, 1998, **37**, 4131.
21 A. Choudhury and S. Natarajan, *Solid State Science*, 2000, **3**, 365.
22 J. Larionova, B. Mombelli, J. Sanchiz and O. Kahn, *Inorg. Chem.*, 1998, **37**, 679; L. O. Atomyan, G. V. Shilov, R. N. Lyubovskaya, E. I. Zhilyaeva, N. S. Ovanesyan, S. I. Pirumova, I. G. Gusakovskaya and Y. G. Morozov, *JETP Lett. Engl. Transl.*, 1993, **58**, 766; S. Decurtins, H. W. Schmalle, H. R. Oswald, A. Linden, J. Ensling, P. Gütlich and A. Hauser, *Inorg. Chim. Acta*, 1994, **216**, 65.
23 J. Glerup, P. A. Goodson, D. J. Hodgson and K. Michelsen, *Inorg. Chem.*, 1995, **34**, 6255; J. Y. Lu, M. A. Lawandy and J. Li, *Inorg. Chem.*, 1999, **38**, 2695.
24 C. W. Yan, Y. T. Li, Y. Z. Su and D. Z. Liao, *Polyhedron*, 1998, **8**, 1311; S. L. Lambert, C. L. Spiro, R. R. Gange and D. N. Hendrickson, *Inorg. Chem.*, 1982, **21**, 68.
25 C. Mathonière, C. J. Nuttall, S. G. Carling and P. Day, *Inorg. Chem.*, 1996, **35**, 1201.
26 M. N. Burnett and C. K. Johnson, ORTEP-III: Oak Ridge Thermal Ellipsoid Plot Program for Crystal Structure Illustrations, Report ORNL-6895, Oak Ridge National Laboratory, Oak Ridge, TN, USA, 1996.